Finite-element method for calculation of the effective permittivity of random inhomogeneous media

Viktor Myroshnychenko and Christian Brosseau*
Laboratoire d'Electronique et Systèmes de Télécommunications (Unité Mixte de Recherche CNRS 6165), Université de Bretagne Occidentale, CS 93837, 6 avenue Le Gorgeu, 29238 Brest Cedex 3, France
(Received 22 March 2004; revised manuscript received 22 September 2004; published 4 January 2005)

The challenge of designing new solid-state materials from calculations performed with the help of computers applied to models of spatial randomness has attracted an increasing amount of interest in recent years. In particular, dispersions of particles in a host matrix are scientifically and technologically important for a variety of reasons. Herein, we report our development of an efficient computer code to calculate the effective (bulk) permittivity of two-phase disordered composite media consisting of hard circular disks made of a lossless dielectric (permittivity ε_2) randomly placed in a plane made of a lossless homogeneous dielectric (permittivity ε_1) at different surface fractions. Specifically, the method is based on (i) a finite-element description of composites in which both the host and the randomly distributed inclusions are isotropic phases, and (ii) an ordinary Monte Carlo sampling. Periodic boundary conditions are employed throughout the simulation and various numbers of disks have been considered in the calculations. From this systematic study, we show how the number of Monte Carlo steps needed to achieve equilibrated distributions of disks increases monotonically with the surface fraction. Furthermore, a detailed study is made of the dependence of the results on a minimum separation distance between disks. Numerical examples are presented to connect the macroscopic property such as the effective permittivity to microstructural characteristics such as the mean coordination number and radial distribution function. In addition, several approximate effective medium theories, exact bounds, exact results for two-dimensional regular arrays, and the exact dilute limit are used to test and validate the finite-element algorithm. Numerical results indicate that the fourth-order bounds provide an excellent estimate of the effective permittivity for a wide range of surface fractions, in accordance with the fact that the bounds become progressively narrower as more microstructural information is incorporated. Future directions of the active field of computational studies of the structure-property relations for composite systems are briefly discussed.

DOI: 10.1103/PhysRevE.71.016701 PACS number(s): 02.70.Dh, 77.22.Ch, 73.40.−c

I. INTRODUCTION AND MOTIVATION

A. Overview

From biology to geology to electronics, a number of materials involve composites. Although some of these materials are found in nature, laboratory processing is often needed for efficient use. Others are entirely synthetic, created by chemical and physical processes. Certain materials are multiphase composites designed for certain desirable response properties otherwise unavailable. With regard to linear macroscopic electromagnetic response of these materials, the inconsistency between theory and experiment emphasizes the prominence of some kind of phenomenology in this problem [1–3]. It might be noted that within a continuum approach, the issue of electromagnetic properties is analogous to the thermal or elastic properties of heterogeneous solids, the permeability of porous media, and the rheology of hydrodynamic suspensions. In recent years, a great deal of effort has been directed towards a fundamental understanding of the effective transport properties of composites that relate average flux fields to average gradient fields [4–6]. Taking into account a great diversity of physical processes, these studies are capable of answering many practically important issues of condensed-matter physics and materials science. However, many models for determining the effective permittivity discussed in the literature are heuristic in nature, applying only to a specific combination of particles-host medium. This is not to say that we have not learned an enormous amount about the dielectric properties of condensed-matter systems, both from experimental and theoretical studies. Considerable controversy surrounds the problem of determining the effective transport properties in composite materials. One important, and as yet not completely answered, question in this area concerns the observed similarities of the permittivity vs volume fraction of inclusion variation among various types of stochastic heterogeneous systems. Each individual system is of course unique unto itself but, consistent with this diversity, there are overall similarities which one would like to explain. On the experimental side, results are being consolidated, mainly due to a considerable improvement in the quality of the samples compared to those used in the early studies of composite materials.

Many theorists have examined this subject by performing *ab initio* calculations, e.g., density-functional theory (DFT) [7], the finite-element method (FEM) [8], the different variants of the boundary integral equation (BIE) [9–11], the first-principles molecular dynamics [12], the finite integration algorithm [13], the Monte Carlo (MC) algorithm [14], multipole moments [15,16], the genetic algorithm [17], the

*Corresponding author. Also at the Département de Physique, Université de Bretagne Occidentale, 29238 Brest Cedex 3, France. FAX: 33-2-98 01 61 31. Email address: brosseau@univ-brest.fr

finite-difference-time-domain (FDTD) method [18], and the fast Fourier transform (FFT) method [19–21], on a variety of systems where only two phases are present. Related to the problem at hand, the notions of random close packing (RCP) and maximally random jamming have been discussed by Torquato and co-workers [22–24]. The main problem is that real calculations are not easy, and the challenge is to find a reasonable balance between the choice of method, desired accuracy, and computational expense. The most desirable approach for fully harnessing the dielectric properties of heterostructures at the macroscale must be inherently multiscale (both in time and space) since its evolution is mediated by a combination of atomic level dynamics, defect physics, nonequilibrium thermodynamics, and transport kinetics. Most numerical analyses reported thus far have fallen short of this goal for a variety of reasons. While numerical approaches may be exact in principle, the true form of the randomness is unknown. The high computational cost of averaging over a large set of system configurations makes it difficult to obtain well-converged estimates of the observables. Current research is pushing available approximations to the description of fluctuations on the hierarchy of length scales which are relevant to the problem. Actually, the cross-fertilization between computational and analytical work in the area of composite materials is quickly growing. Unfortunately, current feasible representations for the *a priori* knowledge of the microstructure of the composite, such as the correlation functions that specify the average microscopic arrangement of the constituents, require significant experience in the construction of reliable and solvable microstructures. The primary reason for the limitation of "exact" calculations of the property of interest, especially for continuum models, has been the lack of efficient algorithms suited to generate collections of random packings of particles (disks, spheres). It is perhaps fair to observe that theories that start with similar algorithms may arrive at different descriptions of their properties. Yet even if this "disorder representation problem" were solved in its entirety, the would-be-composite designer would still face the formidable tasks of (1) finding the starting entities that will maintain their structural integrity throughout the synthesis process, and (2) controlling the morphology he or she wished to engineer. As testimony to these difficulties, it is not uncommon to find in the literature disagreements over the predictions of the porosity, mean coordination number, and radial distribution function [22,25]. We will return to this point later. But let us take a step backward and discuss the effective-medium approach within continuum models.

B. Basic facts about the effective-medium approximation

For decades, other theorists have developed approximate analytical theories to describe the electromagnetic properties of macroscopically inhomogeneous media. The main thrust of this field has so far been extensive exploration of their applications, although some of their fundamental properties were characterized experimentally. Given the empirical nature of calculations of the complex effective permittivity of disordered materials, and the lack of direct comparison with experiments for validation, first principles *ab initio* calculations are an issue at the core of contemporary condensed-matter research. Physicists have been engaged in this area at least since Maxwell [26] (in particular, his method for calculating the conductivity of a simple-cubic lattice of spherical inclusions), but it was not until the 1930s, primarily under the influence of Bruggeman's pioneering work [27], that there was a systematic attempt to establish the foundations of the self-consistent effective-medium approach and bring it into the physical mainstream. As already pointed out, effective-medium theories (EMT) and generalized effective-medium theories (GEMT), as well as other mean-field-like approximations [28–30], are believed to represent the gross features of the electromagnetic behavior of heterostructures. In general, this is done by averaging all pertinent variables such as the induction field vector and the permittivity over the composite medium viewed as a continuum consisting of a matrix with inclusions. This suggests that, in the long-wavelength limit, the observed bulk material should be described (almost) completely by an "effective" permittivity. What precisely this "effective" approach really entails is still a controversial issue (see, e.g., Refs. [6,22,31]). Recent very detailed numerical calculations by Brosseau and Beroual [9] for regular arrays, i.e., translationally invariant, of 2D and 3D inclusions embedded in a uniform matrix, indicate that the spatial arrangement of the constituents in the mixture is reflected in the manner in which local fields are established. Despite the status of periodic systems as benchmark materials for the study of composites, many aspects of the physics of composites require better theoretical explanation and still inspire a wealth of interesting ongoing research [28,29].

While these EMT have greatly advanced our understanding of wave transport in heterogeneous materials at a fundamental level, their ability to make quantitative predictions is still somewhat limited due to the lack of model microstructures that can accurately represent actual materials of interest, i.e., impracticability of any approach based on knowing the full topology of the system. A real composite system must ultimately be described statistically through the specifications of an infinite set of multipoint correlation functions which characterize the microstructure of the two-phase medium [6,24,32]. A comprehensive discussion of these microstructured correlation functions can be found in the books by Torquato [24] and Milton [6], and we refer the reader to these texts for further specifics. It has been argued that a serious issue (regarding inverse transformation problems in general) is that while the effective permittivity can be determined for a particular microgeometry, the reverse problem is ill-conditioned in the sense that many different microstructures could produce the same permittivity data. Another objection to EMT is that they do not allow for the spatial correlations between the inclusions, i.e., each component is surrounded by the same effective medium [29]. Limitations of the earlier dipolar approach have called for an extensive renewal of the enabling theoretical and experimental methodology towards modeling transport properties by taking into account the multipolar character of the particle-particle interactions [32]. The shortcomings of the above methods have been dealt with to some extent through combined approaches (see, e.g., [33]) and improved strategies for estimating the important parameters characterizing the electromagnetic transport through disordered materials.

C. Motivation and plan of the paper

In the current work, we introduce a finite-element method (FEM) for calculating the effective permittivity of macroscopically inhomogeneous media. This paper is the first installment of that study and is exclusively dedicated to generic two-dimensional (2D) two-phase heterostructures consisting of hard circular disk equilibrated distributions [34]. Other papers in our study will focus on the study of the permittivity behavior for 3D models and composites near percolation threshold. The hard-disk distribution has been chosen as the reference system since it is one of the simplest idealized models to explain structural and kinetic properties of matter [34–39], e.g., disk configurations in the plane have been advanced as a simple model for the arrangements of particles adsorbed on smooth surfaces [40,41]. Such systems can be in thermal equilibrium or in one of the many nonequilibrium states. While particles in equilibrium have thermal motion such that they sample the configuration space uniformly, particles in nonequilibrium states usually do not sample the configuration space uniformly, since they do not diffuse after they have been placed into the system [24]. The primary purpose of this paper is to present a practical algorithm for calculating the effective permittivity ε of a random 2D statistically isotropic composite in equilibrium consisting of impenetrable circular disks of phase 2, with permittivity ε_2 and surface fraction ϕ_2, randomly dispersed in a matrix of another dielectric phase, say 1, with permittivity ε_1 and surface fraction $\phi_1 = 1 - \phi_2$. The 3D analog of this model would be a composite consisting of parallel infinitely long and equisized cylinders with circular cross sections of phase 2 inserted in the phase 1, i.e., all interfaces are parallel to a fixed direction. Such a composite has a transversally isotropic symmetry and the dielectric properties can be described by two parameters, one corresponding to the direction of fibers and another one corresponding to the transverse direction. While the value of effective permittivity in the direction of fibers can be found exactly [29], i.e., $\varepsilon_L = \varepsilon_1\phi_1 + \varepsilon_2\phi_2$, finding the transverse component is a more difficult task. A number of earlier works [13,18,22] have considered a numerical approach to this problem. These early investigations focus on modeling the effective conductivity of several systems including the case of 2D regular arrays of perfectly conducting disks. It would be beneficial to determine *both* the structural parameters and the dielectric characteristics within the same numerical scheme. Given the importance of models of two-phase materials, there is a need for systematic investigation of how the randomness and connectedness influence the effective permittivity. The major purpose of this paper is to contribute to the investigation of the structure property for such systems by computer simulations. This kind of information is required for identifying the mechanisms of polarization and conduction in real systems, e.g., thin films made by sputtering by ion bombardment often have a columnar structure, similar to what we consider here. Here, we will consider a two-step calculation process. On the one hand, we generate the random medium using a MC method. Disk packings are created by placing a number of particles within a square cell with periodic boundary conditions. On the other hand, we get the effective permittivity using a FEM-based numerical method. In this paper, we show that our method is generally applicable to various continuum systems and accurately improves the estimate for the effective permittivity of continuum media where local permittivity varies randomly from point to point.

The remainder of this paper is structured as follows. Section II outlines the basic computational framework and a description of the simulation details in terms of which the problem of calculating the "effective" permittivity of inhomogeneous two-phase materials can be approached. The explicit numerical results from our simulations of well-equilibrated random distributions of equal-sized disks are summarized in Sec. III. We consider a number of test cases to demonstrate the utility of our method. Calculations performed in this section permit us to test the validity of this numerical scheme by comparison with upper and lower bounds on the effective permittivity, and with results obtained from conventional EMT. The paper is concluded in Sec. IV with a summary of our results, of possible future applications of the numerical approach developed here, and of some open questions.

II. NUMERICAL IMPLEMENTATION

Over the past two decades, computer simulation has proved itself to be a valuable tool, offering insights into the relationship between the dielectric properties of multiphase composites and their microstructure, an issue of central importance in condensed-matter research due to the wide variety of heterostructures which exist in practice.

A. Two-phase microstructure

Two approaches have received wide recognition in the theory of random heterogeneous material. In the first approach, the microgeometry may be chosen to follow as closely as possible the phase arrangement of a given sample of the material to be modeled, obtained, e.g., from transmission electron microscopy images. The resulting description is called a "real structure" model [9,24,42]. The structure analysis in such materials is complicated due to the presence of the multitude of length scales, and because the experimental probes used have different, and often limited, space and time resolution. In addition, there are certain problems with the interpretation of the images [43]. Consequently, all this (partial) information is insufficient for uniquely finding a model for the microstructure. The second approach is based on statistically based algorithms for reconstructing the microgeometry. This approach allows systems with both arbitrary shapes and arbitrary dielectric characteristics to be considered. In the current work, we shall use a probabilistic model to represent such "numerical structure."

The traditional METROPOLIS sampling [24,44] scheme is adapted to generate equilibrated sets of realizations for the statistically homogeneous and isotropic composite which is studied. The basic parameters in this model simulation are the length L of the square primitive cell side, the number N of hard disks, their diameter D, and their surface fraction ϕ_2. The following is a brief explanation of the key steps of this

algorithm. First, an initial configuration of particles in a unit cell is generated. We used a random starting configuration which enables us to attain more rapidly equilibrated sample realizations. Depending on the value of ϕ_2, different strategies for random placing are used.

For small values of ϕ_2, we use the random sequential addition (RSA) process [45] because it is fast and easily implemented on a computer. The procedure starts by positioning the desired number of particles randomly (using a uniform distribution) and sequentially in the initially empty square cell. If a particle can be placed into the square cell without overlapping with other disks, then it remains fixed at this position throughout the simulation. If the particle overlaps another existing particle in the cell, then another attempt is made until a nonoverlapping location can be found. As this acception and rejection process continues, it becomes more difficult to find available regions into which the disk can be added, and in the saturation limit (for monodisperse circular disks, $\phi_2^{\mathrm{sat}} \cong 0.55$), no further addition is possible and the process is over.

For $\phi_2 > \phi_2^{\mathrm{sat}}$, an alternative approach is used for generating the initial configuration which is based on the Clarke and Wiley collective rearrangement method that was initially developed for generation of a random close packing of hard spheres [46]. At the start, a required number of particles are randomly placed inside a square cell according a uniform distribution. In general, there will be steric overlaps among the disks. To reduce these overlaps, the disks are then moved one at a time along the vector sum of the overlaps. Moving a disk along the vector sum of the overlaps may reduce or eliminate some overlaps but will create or increase others. To avoid increasing overlaps, a move is accepted if it does not create any overlap larger than the maximum overlap among all the disks. Thus, the maximum overlap always decreases or remains constant. If the move is not accepted for a particular disk, the disk is moved again in the same direction by a smaller amount. If this operation is not successful after a few attempts, the disk is given a small random displacement. Again the move is accepted or rejected depending on whether the maximum overlap is less than or greater than the maximum overlap among all the disks. Each disk in the packing is moved sequentially in this way until there are no more overlaps. Sometimes any disk may be locked into its position, i.e., it cannot be moved without creating an overlap equal to or less than the maximum overlap among all disks. In this case, all disks are vibrated by giving to each disk a small random displacement and the process is continued.

After an initial configuration is generated, MC cycles are started in order to drive the system to equilibrium. At each MC step, one attempts to move randomly the center-of-mass coordinate of each disk. The new configuration is accepted if the particle does not overlap with any other particles. If the attempted move causes an overlap, the particle is not moved and the new configuration is the same as the old one. The maximum amplitude of the MC moves is adjusted to give an approximately 50% acceptance ratio. This process is repeated until equilibrium is achieved, i.e., when the pair correlation function does not change with time. In order to minimize boundary effects due to the finite size of the system, periodic boundary conditions are employed in the present simulation. This means that the unit cell containing the particles is repeated periodically within the plane to form an infinite lattice. With an infinite number of particles in the unit cell, the METROPOLIS algorithm produces statistically homogeneous and isotropic equilibrated ensembles of hard circular disks.

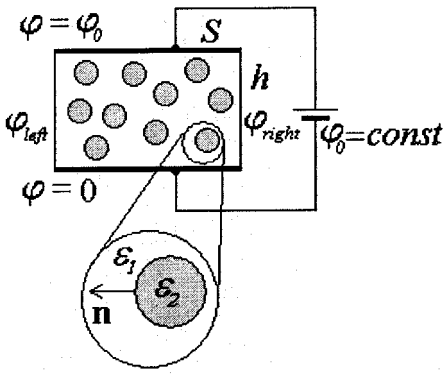

FIG. 1. Illustration of the calculation of the effective permittivity of composite.

For completeness, it is worth observing that other procedures for generating random particle packings were described in the literature [24,47–52], to which the reader is referred for additional information.

B. Model of the effective permittivity and its basic equations

To investigate in some detail the dielectric properties of heterostructures in the quasistatic limit, a method suitable for determining the effective permittivity is needed. A detailed description of the method can be found elsewhere [53], though the relevant relations are included in this subsection. An illustration is useful at this point.

Figure 1 shows that we consider a parallel plate capacitor, with conducting plates of area S and separation distance h which is filled with the composite medium to be studied. The macroscopically inhomogeneous medium consists of two types of isotropic dielectric materials, 1 and 2, with permittivities ε_1 and ε_2, respectively. Here the permittivity ε is a relative quantity compared to the free space permittivity $\varepsilon_0 = 8.85 \times 10^{-12}$ F m^{-1}. A constant potential difference φ_0 is kept between the capacitor plates. Assuming that h is small enough so that fringing effects can be ignored, then the effective permittivity ε of the composite can be determined from the energy W stored in the capacitor as

$$W = \frac{1}{2}\varepsilon_0 \varepsilon \frac{S}{h}\varphi_0^2, \tag{2.1}$$

where $\varepsilon_0 = 8.85 \times 10^{-12}$ F m^{-1} is the permittivity of the vacuum. This definition ensures us that the energy stored in the capacitor would be the same if the composite medium was replaced by a homogeneous medium with permittivity ε subject to the same boundary conditions. The energy W can also be expressed in terms of the spatial distribution of the electrostatic potential $\varphi(\mathbf{r})$ inside the capacitor if the microscopic structure of the material is known. Since the compos-

ite considered here is locally isotropic, the energy W is

$$W = \frac{1}{2}\varepsilon_0 \int_{\Omega} \varepsilon(\mathbf{r})[\nabla \varphi(\mathbf{r})]^2 d^2\mathbf{r}, \tag{2.2}$$

where $\varepsilon(\mathbf{r})$ is the local dielectric constant, where the integral in Eq. (2.2) extends over the surface Ω of the capacitor. Thus, determining the effective permittivity of the composite medium requires knowledge of the distribution of the local electrostatic potential $\varphi(\mathbf{r})$.

For that purpose, one can solve the following boundary-value problem:

$$\nabla \cdot [\varepsilon(\mathbf{r}) \nabla \varphi(\mathbf{r})] = 0 \tag{2.3}$$

in conjunction with the boundary conditions $\varphi_{bottom}=0$ at the bottom plate and $\varphi_{top}=\varphi_0$ at the top plate. Edge fringing effects can be eliminated by the periodic extension of the capacitor. For that purpose, we apply periodic boundary conditions on the left and right boundaries of the unit cell. Periodic boundary conditions mean that the two boundaries should be treated as identical. Two conditions are required: (1) it must be possible to transform opposite faces into each other by a simple translation, and (2) for each pair of faces the phase distributions and the FE discretization must be compatible. In addition, the potential and its derivatives are supposed to be continuous along a line that approaches the right boundary from inside the domain, jumps to the corresponding location on the left boundary and from there continues into the domain. Stated in other words, it requires that the cells together with boundary conditions prescribed on them generate valid tilings both for the geometry and the potential φ. To achieve this, the potential is constrained to have equal values in corresponding points on the left and right boundaries of the unit cell, i.e., $\varphi_{left}=\varphi_{right}$. It should be noted that though our unit cell is periodic in two directions, periodic boundary conditions can be applied just in one of them and consequently the potential will be periodic in one direction. We note also that for simple square and hexagonal unit cells in which the faces of the cell coincide with symmetry planes of the phase arrangement, i.e., the unit cell exhibits a plane of symmetry both for material properties and geometry, periodic boundary conditions simplify to symmetry boundary conditions expressed by the condition $\mathbf{n}\cdot\nabla\varphi=0$ at the edge planes. On any interface between regions of 1 and 2 materials, the potential and the normal component of the displacement vector are continuous, i.e., $\varphi_1=\varphi_2$ on $\partial\Sigma$ and $\varepsilon_1\mathbf{n}\cdot\nabla\varphi_1=\varepsilon_2\mathbf{n}\cdot\nabla\varphi_2$ on $\partial\Sigma$, where the superscripts 1 and 2 label the two regions separated by the interface $\partial\Sigma$, and the vector $\mathbf{n}$ is normal to $\partial\Sigma$.

C. Representative surface element

With such numerical computation, the hard work comes in addressing the issue of the representativeness of the finite surface of the composite that is required for describing its effective dielectric properties. A careful examination of this problem is done in this subsection. It should be mentioned that in the study of a periodic composite, the investigation may be limited to an elementary cell of the periodic structure without loss of information or generality. However, a random composite cannot be characterized by a simple periodic cell, and the study concerns a finite size of the system. Thus an approximation should be introduced. The physical idea is actually quite simple: it is based on the substitution of the composite by its representative surface element (RSE). The analysis is in fact performed on the RSE instead of the whole composite sample. In practical terms, the candidate RSE should be a surface of the composite material that is structurally typical of the whole composite on average, small enough from a macroscopical point of view, but sufficiently large compared to the characteristic scales of the microstructure in order to contain a large number of single inhomogeneities (particles). In this sense, the RSE is statistically representative of the microgeometry of the composite material. But even with this definition, the size of the problem can be too large from the numerical standpoint. To avoid this problem and to satisfy the aforementioned conditions, a cell of "reasonable" size is constructed and periodicity of such cell is assumed. Then, the ensemble-average (effective) permittivity of the composite is found by averaging over many realizations of the structure of the system, i.e., $\varepsilon=(1/\Lambda)\Sigma_{i=1}^{\Lambda}\varepsilon^i$, where Λ denotes the number of realizations and ε^i is the effective permittivity of a particular realization. In like fashion, the variance of the permittivity is given by $\mathrm{var}\,\varepsilon=(1/\Lambda)\Sigma_{i=1}^{\Lambda}(\varepsilon^i-\varepsilon)^2$.

It has to be noted that in the case of an infinite number of particles in the unit cell, the METROPOLIS algorithm would produce an isotropic material. Consequently, a single value of the effective permittivity suffices to describe the dielectric behavior. But here since we consider a finite number of particles, the unit cell is anisotropic. We have directed the coordinate axes along the unit-cell continuation vectors, and for each equilibrated realization, the values of effective permittivity in the x and y directions, respectively, have been calculated. We assume that the value of ε^i, in the above expression of ε, is the average of these two values.

One additional issue that needs to be addressed concerns the unit-cell construction scheme used in the current work, which requires that particle-particle contact be avoided, i.e., there is always a minimum allowable separation distance δ between disks. Why is it that δ is so important? In many experimental approaches to dispersion and self-assembly of nanoscale colloids, surfactant in the form of oligomers or polymers is added in order to improve dispersability or to control the onset of self-assembly. Thus this geometric parameter, δ, can play a role to describe encapsulation of the inclusions. One natural explanation is that connections between particles form singular geometries and the automatic mesh generator may produce very thin triangles when they approach the sharp corners of the geometry (at the points of contact), leading to poor element quality and as a result yielding a large numerical error. On the other hand, when the distances between particles are too small, it becomes impossible to construct and mesh such RSE's. It should perhaps be emphasized in this context that even if RSE's could be constructed and meshed, it would produce a very large number of triangles. Consequently, a solution of the FEM system of equations would be prohibitive in terms of computational cost. To circumvent these complications, we consider the

idealized problem obtained by this no-contact requirement between inclusions. Thus, the particle contact artifacts caused by discretization errors can be avoided. In general, this constraint has the effect of producing an underestimate of the effective permittivity, especially for high surface fractions of inclusions. The physical reason comes from the fact that particle contacts which form connected clusters leading to significant potential-bridging store the large energy concentration and, in turn, strongly influence the effective permittivity. Allowing a larger minimal distance between particles will give lower values of effective permittivity. The point that needs to be kept in mind is the fact that there is no universal optimum value for the parameter δ. Different unit-cell construction schemes lead to different optimum values, even for the simple case of disks. These considerations indicate that the value of δ has to be chosen carefully. It must permit RSE's to be constructed and the energy concentration at the interface of particles to be simulated adequately with a high degree of mesh discretization; simultaneously, the size of the numerical problem should be in a diapason of our computational power. Hence, for numerical efficiency, it is extremely important to determine an appropriate RSE for high permittivity contrast and high surface fraction that has the optimal size and number of particles.

D. Further computational details

To summarize and to aid in the implementation, our self-consistent procedure for the calculation of the effective properties of a random composite is as follows.

(1) Generate randomly distributed disk configurations without overlap in a square box for a specified disk surface fraction and permittivity of each component, using the standard METROPOLIS MC algorithm [34,44]. A periodic square unit cell of constant size $L=1$ was taken in all calculations. The number of disks in the unit cell varied from 16 for $\phi_2=0.10$ to 134 for $\phi_2=0.85$ (Fig. 2). The dependence of the permittivity on disk diameter is shown in Fig. 3(a). We observe a good convergence for $\phi_2<0.4$. During all the runs, the higher ϕ_2, the smaller D is required to achieve convergence. We explored a number of uniform disk diameters between 0.089 and 0.357, and we found that convergence is not obtained for large values of ϕ_2. In Fig. 3(b), the variance of the permittivity is plotted as a function of ϕ_2 for different values of D. It should be stressed that the variance increases as D is increased. In addition, we observe that the sensitivity of the results to D is more pronounced at higher values of ϕ_2 than at lower values. The physical reason is that contacts between disks form connected clusters leading to significant potential-bridging, which corresponds to high electrostatic energy (hot spot) and greatly influences the value of ε. However, this effect is counterbalanced by the influence of the distance δ between particles, i.e., increasing the number of disks in the cell has the effect of increasing the number of gaps and thus ε decreases. We found by a trial-and-error approach that $\delta=0.0005$ was a good compromise: it allows us to construct and mesh unit cells and simultaneously to obtain systems of equations which are in diapason of our computational power. In the calculations discussed below,

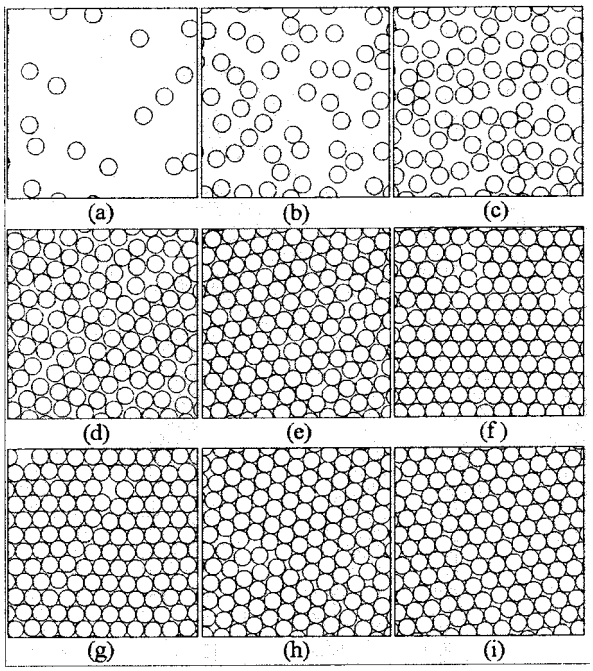

FIG. 2. Typical equilibrium configurations (sample realizations) of the two-phase composite consisting of monodisperse circular disks randomly distributed within a square primitive cell. The sample packing results from the sequential algorithm described in the text applied to a binary mixture with a given surface fraction of disks. (a) $\phi_2=0.1$, (b) $\phi_2=0.3$, (c) $\phi_2=0.5$, (d) $\phi_2=0.6$, (e) $\phi_2=0.7$, (f) $\phi_2=0.8$, (g) $\phi_2=0.82$, (h) $\phi_2=0.83$, and (i) $\phi_2=0.85$.

and unless otherwise stated, the disk diameter was maintained constant at $D=0.09$. We were able to model dense monodisperse circular disk configurations with a particle surface fraction up to $\phi_2^{\max}\cong 0.85$. It is worthy of note that this value agrees well with the estimates of the RCP of hard disks which have been published in the literature [35,50,54–59]. The ensemble average was done over 100 realizations. The number of MC steps N_{MC} needed to achieve equilibrium depends on ϕ_2 and will be discussed in Sec. III. The generation of the random numbers was done by an internal MATLAB function which uses a lagged Fibonacci random numbers generator, with a cache of 32 floating point numbers, combined with a shift register random integer generator [60,61].

(2) Carry out the calculation of the effective permittivity using the FEM software package FEMLAB [62] with the aid of MATLAB environment [60]. FEMLAB has an automatic mesh generator which uses a Delaunay algorithm and has many parameters for controlling the size and the density of the element in the mesh. Quadratic triangular elements were used for discretization of the unit cell. It should be noted that the meshing of our model domain takes into account the border between the matrix and disks, i.e., the mesh is automatically adjusted to conform with substantial changes of the material parameters. The number of nodes used in the calculations depends on the surface fraction of disks, e.g., it is about 5000 for small surface fraction to about 100 000 for the highest surface fractions. The effective permittivities in the x and y directions are found for each realization by applying a unit potential, $\varphi_0=1$ V, in the corresponding directions with the same boundary conditions.

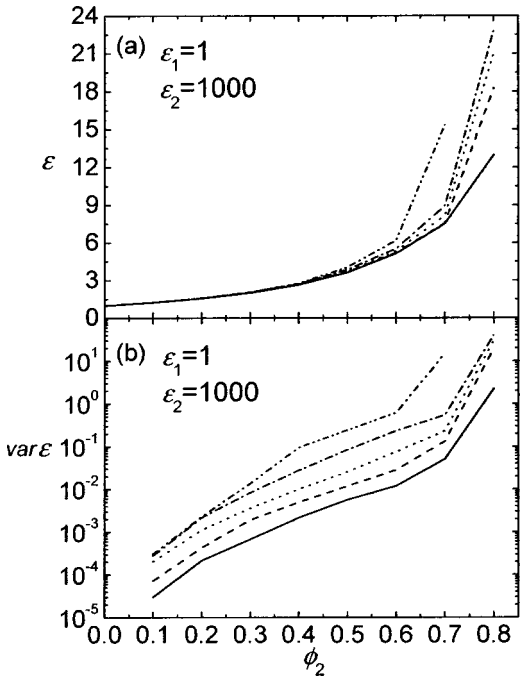

FIG. 3. (a) The dependence of the effective permittivity as a function of ϕ_2 for random configurations of disks with $\varepsilon_1=1$ and $\varepsilon_2=1000$. Dash-dot-dotted, dash-dotted, dotted, dashed, and solid curves correspond to $D=0.357$, $D=0.252$, $D=0.178$, $D=0.126$, and $D=0.089$, respectively. (b) Same as in (a) for the variance of the effective permittivity.

(3) Average the effective permittivity of the composite structure over all sample realizations. All calculations were carried out on a 2.4 GHz Intel Pentium 4 system running Windows.

III. RESULTS AND DISCUSSION

To illustrate how the numerical scheme described above works in practice, we performed repeated calculations for various surface fractions and permittivity ratios. Here we show the results for structural aspects in terms of the radial distribution function and the mean coordination number, i.e., the number of inclusions in contact with a considered inclusion. In order to test the code and validate the method, we calculated the effective permittivity of binary mixtures of hard disks and compared the numerical results with those obtained from conventional EMT and predictions from bounds.

A. Radial distribution function $g_2(r)$

There are many statistical descriptors of a random heterogeneous material defined by an ensemble of many-particle systems. For statistically homogeneous media, the most basic statistical descriptor which provides structural information about the equilibrium system is the radial distribution function (RDF). It should be recalled that whereas the properties of a hard-rod ($d=1$) system are known exactly [63], not a single exact result is known when $d\neq 1$. Consequently, one resorts to some approximate integral equation for the structural correlation functions, e.g., the Percus-Yevick (PY) equation. The RDF for hard disks has been largely studied in the literature [24,64], but unfortunately the PY equation cannot be solved analytically for $d=2$.

The RDF is usually referred to as the pair correlation function, which describes how, on average, the particles in a system are radially packed around each other. It is defined as the probability of finding one disk center at a given distance r from the center of a reference disk. Within the computer simulation, it can be obtained by generating a histogram in the following manner [24]. The surface around each disk is divided into concentric shells of finite thickness Δr, and the number of disks in each shell $n(r)$ at radial distance r is counted and divided by the shell surface $v_{shell}(r)$ to obtain the local density. The radial distance r is assumed to be midway between the inner radius $r-\Delta r/2$ and outer radius $r+\Delta r/2$ of the shell. To obtain $g_2(r)$, the densities at each distance are then averaged over all particles and normalized to the number density of particles, i.e., ρ. The statistically isotropic medium considered here implies that the r dependence of the RDF is given by

$$g_2(r)=\frac{n(r)}{N\rho v_{shell}}. \tag{3.1}$$

To obtain a reliable statistics, $g_2(r)$ is calculated by taking an average over many generated configurations. In this work, Δr was set to $0.1D$.

Figures 4(a)–4(d) display the influences of the reduced radial distance and number of MC steps on the RDF when the surface fraction of disks is held fixed. How well are the resulting configurations equilibrated? The quality of the equilibration can be judged from the evolution of the RDF's as N_{MC} is varied. The number of MC steps required to achieve equilibrium increases as ϕ_2 increases from typically 10 for $\phi_2=0.3$ to 3000 for $\phi_2=0.7$ to 10 000 and more for $\phi_2\geqslant 0.8$. This panel of figures exhibits two remarkable features of the RDF's. First, the first peak is the highest in the RDF's for all surface fractions. The "periodicity" of the peaks is governed by the diameter of disks. Additionally, it can be noticed that as ϕ_2 increases, spatial correlations build up and lead to nontrivial structure in $g_2(r)$: the first peak is slightly displaced to smaller distance. Second, as the RCP surface fraction for equilibrated distributions is approached, larger fluctuations in the peaks of the RDF appear. This affects qualitatively the shape of the RDF profile that now exhibits oscillatory behavior.

We have also looked at the RDF of the random configurations of disks that we generate for our simulations and compared them to the distribution function of a mixture of hard disks, as predicted from solution of the PY integral equation. Figures 5(a)–5(d) depict the observed and predicted $g_2(r)$. What is interesting is that the results are practically indistinguishable for $\phi_2<0.69$ over the whole range of r/D, but the most glaring difference between PY theory and simulation arises for $\phi_2>0.7$. For such a case, the PY theory does not accurately capture the positions of the peaks in the RDF, in agreement with the fact that $\phi_2=0.7$ is slightly higher than the surface fraction at which an ordering transi-

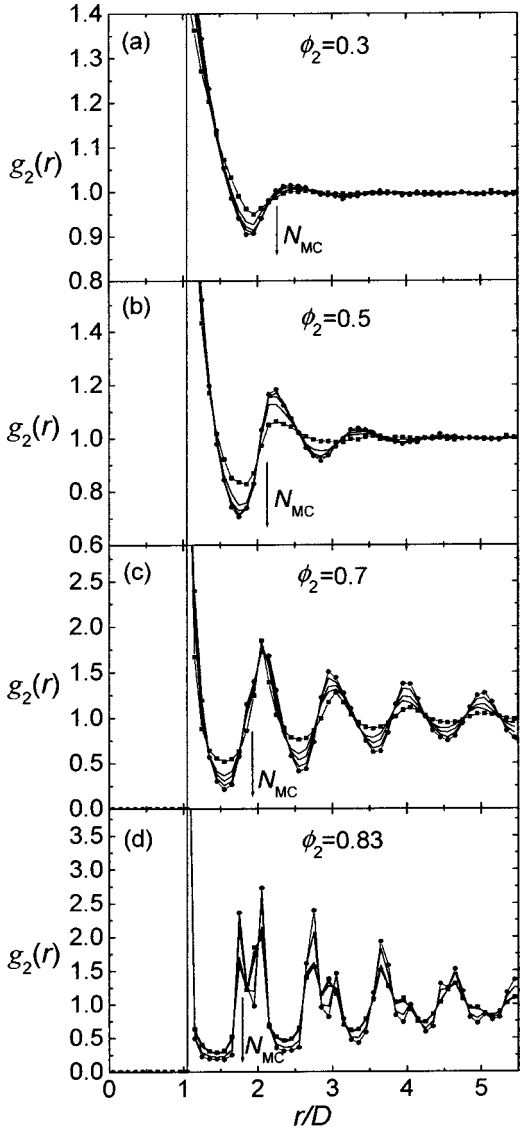

FIG. 4. The dependence of the radial distribution function $g_2(r)$ hard disks as a function of the dimensionless radial distance r/D for different surface fractions of disks. $D=0.045$. The filled squares are simulation data for a nonequilibrium system, the solid curves are evolution of systems at various stages of the equilibration procedure, i.e., for different values of N_{MC} ranging from a few tens to a few 10^4, and the filled circles are simulation data for the hard disks system in equilibrium. The arrow indicates the evolution of the profiles of $g_2(r)$ as N_{MC} steps are increased. (a) $\phi_2=0.3$, (b) $\phi_2=0.5$, (c) $\phi_2=0.7$, and (d) $\phi_2=0.83$.

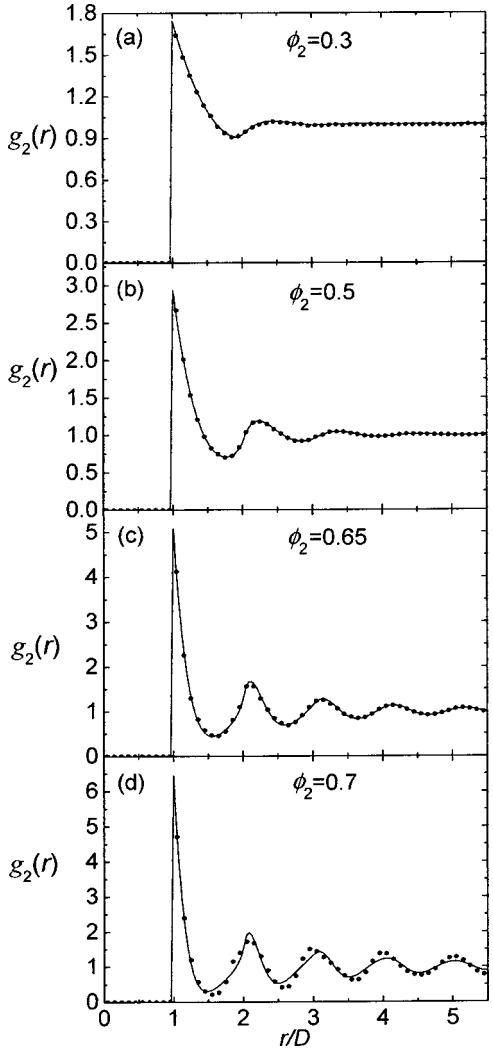

FIG. 5. The dependence of the radial distribution function $g_2(r)$ hard disks as a function of the dimensionless radial distance r/D for different surface fractions of disks. For comparison, the solid curve shows the corresponding values of the RDF calculated within the Percus-Yevick approximation. (a) $\phi_2=0.3$, (b) $\phi_2=0.5$, (c) $\phi_2=0.65$, and (d) $\phi_2=0.7$.

tion is expected to appear [22]; $\phi_2>0.7$ correspond to metastable disordered, i.e., glassy, states for which the RCP fraction has been found to be ≈ 0.82 [35].

The last point we want to focus on in this discussion concerns the long-ranged behavior of the correlations in the critical region near the RCP fraction. Tobochnik and Chapin [65] and Song and co-workers [66] have argued that $g_2(r=D)$ diverges for ϕ_2 near ϕ_{2c} according to a power law, i.e., $g_2(D)\sim(\phi_{2c}-\phi_2)^{-s}$ with $s=1$ for $d=2$ and 3. In Fig. 6, we show our prediction of the $g_2(r)$ data for $r/D=1$ versus $\phi_{2c}-\phi_2$ in a semilogarithm plot. The data do fall reasonably on a line over the limited range of data used. Our prediction of $s=1.010\pm0.016$ is very close to unity in the limit that $\phi_2\rightarrow\phi_{2c}$. Here $\phi_{2c}=0.862$.

B. Mean coordination number

The resulting packing structures are also analyzed in terms of mean coordination number Z. Mean coordination number is defined as the average number of disks in contact with a considered disk. It should be noted that Z is very sensitive to the definition of "contact" or critical distance, i.e., the minimal distance between two disks before they are regarded to be in contact. In 2D, we have the following obvious steric constraint: $Z\leqslant 6$.

Because the constraint of a minimum allowable separation distance between disks is an artifact, we also looked at the effect of this parameter on Z. In Fig. 7, the computed

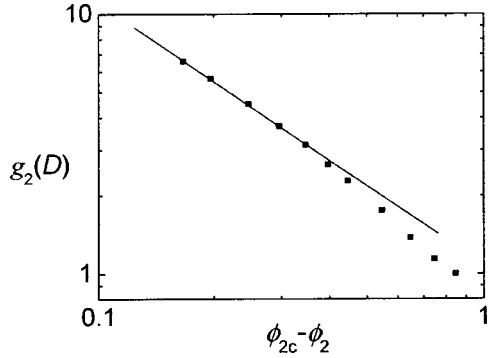

FIG. 6. Scaling plot of the RDF as a function of $\phi_2^{\max} - \phi_2$. Here $r/D=1$.

values of Z of the hard-disk system are shown as a function of the surface fraction of disks and δ. Expectedly, the mean coordination number increases monotonically as a function of ϕ_2. Upon an increase of the parameter δ, the effective permittivity increases. In all cases (not shown), we observed a similar trend as displayed in Fig. 7. We mention that our results for Z are in close agreement with those obtained in previous simulation studies [22,31]. The increase in Z has the effect of enhancing the polarization of the inclusions.

C. Effect of phase interchange and duality relations

The previous subsections described procedures that constitute the structural stage of these simulations. The present, and following, subsections discuss how equilibrated arrangements of disks affect the effective permittivity.

Keller [67], and Dykhne [68] showed more than three decades ago that continuum composites with a 2D microgeometry have a specific symmetry, namely the duality. The generalization of these duality relations, e.g., to the case of general anisotropic permittivity tensors, has been given by a number of authors including Mendelson [69], Balagurov [70], Milton [71], Durand [72], and Schulgasser [73]. It is worth noting that the duality (or phase exchange) relation was first derived in terms of conductivity [2,33], but for reasons of consistency, we treat it, in the present work, in terms of permittivity. It can be applied to any 2D two-phase composite as long as the x and y axes are the principal axes of the effective permittivity tensor, i.e., regardless of the phase geometry. It states that the effective permittivity determined in the x direction for a medium in which the inclusions (the matrix) have permittivity ε_1 (ε_2), $\varepsilon^x(\varepsilon_1,\varepsilon_2)$, is related to the effective permittivity of the phase-interchanged composite in the y direction, $\varepsilon^y(\varepsilon_2,\varepsilon_1)$, independently of the specific structure by the following equation:

$$\varepsilon^x(\varepsilon_1,\varepsilon_2)\varepsilon^y(\varepsilon_2,\varepsilon_1) = \varepsilon_1\varepsilon_2. \tag{3.2}$$

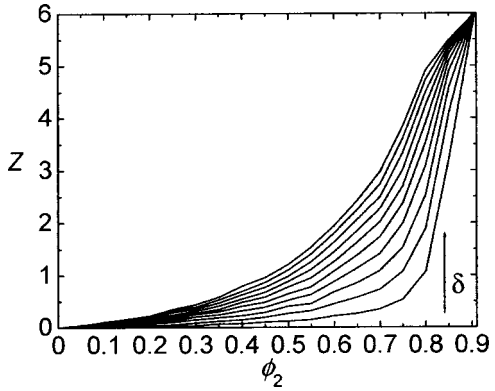

FIG. 7. The dependence of the mean coordination number Z vs surface fraction of disks at varying the minimum separation distance δ allowed between disks from 0.001 to 0.01 with step equal to 0.001.

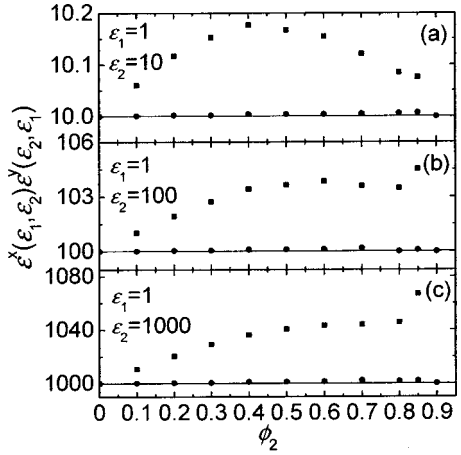

FIG. 8. Comparison of our FEM data for ε with those obtained from Eq. (3.2). Solid squares (circles) correspond to FEM data with applied periodic (symmetry) boundary conditions. (a) $\varepsilon_1=1$, $\varepsilon_2=10$, (b) $\varepsilon_1=1$, $\varepsilon_2=100$, and (c) $\varepsilon_1=1$, $\varepsilon_2=1000$.

Before checking Eq. (3.2) with our results, we first note that a problem arises due to the fact that we have calculated effective permittivity ε^x (ε^y) in direction x (y) with periodic boundary conditions applied just along axis y (x). It means that actually we have calculated effective permittivity ε^x (ε^y) of a thin layer of the composite system in direction y (x), and consequently, Eq. (3.2) cannot be used directly for comparison with our results. Note that the calculated effective permittivity incorporates information about 2D periodicity because it is averaged over ε^x and ε^y. For our purpose, we carried out calculations of the ensemble-average permittivity of the same system but when symmetry boundary conditions are applied to the lateral side of the periodic cell, i.e., we restrict our calculation to a unit cell without taking into account periodicity. Thus we fulfill requirements of Eq. (3.2).

Comparison of the FEM results with those obtained from Eq. (3.2) is displayed in Fig. 8 for cases when periodic and symmetry boundary conditions are applied. As can be seen from Fig. 8, our results with symmetry boundary conditions are in excellent agreement with relation (3.2). Another observation is that ε corresponding to cells with applied periodic boundary conditions is higher than the corresponding value of ε for cells with applied symmetry boundary conditions because in this case the FEM scheme takes into account the interaction between particles of neighbor cells while symmetry boundary conditions do not "see" these particles.

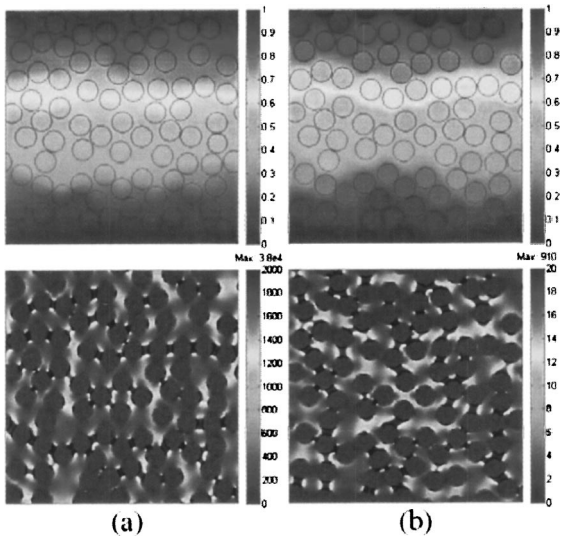

FIG. 9. Schematic of the FEM-calculated electrostatic potential (top) and energy (bottom) in the unit cell with surface fraction of hard disks $\phi_2=0.5$. (a) $\varepsilon_1=1000$, $\varepsilon_2=1$; (b) $\varepsilon_1=1$, $\varepsilon_2=1000$. The bars on the right give the values of the potential and the energy corresponding to the graytones.

As an aside to these calculations, Figs. 9(a) and 9(b) show the electrostatic potential and energy for two types of mixtures: (a) when the inclusion permittivity is lower than the matrix permittivity $\varepsilon_2/\varepsilon_1 \ll 1$, and (b) an inverted mixture where the inclusion permittivity is higher than the matrix permittivity $\varepsilon_2/\varepsilon_1 \gg 1$. These graphs, which provide information on the variation of the local electric field, reveal the presence of regions of high field intensity inside the composite. The energy in such systems flows along trajectories (chainlike structures), avoiding low-permittivity regions in favor of regions where the permittivity is high.

D. Upper and lower bounds on the effective permittivity

As was recalled in the Introduction, the determination of the effective permittivity necessitates knowing an infinite set of correlation functions which statistically characterize the microstructure of the two-phase medium. However, in practice such a complete statistical characterization of the medium is almost never known. Given limited microstructural information on the composite, a number of upper and lower bounds on the effective permittivity (conductivity) have been derived using variational principles [6,24,29,74–76]. For example, optimal second-order bounds, i.e., Eq. (A2), which apply to any composite material with two isotropic components, were established by Hashin and Shtrikman in 1962 [74]. Over the years, progressively tighter bounds have emerged, e.g., Eqs. (A3) and (A4). In this area, we note the work of Silnutzer [77] and Milton [71] for any isotropic two-phase material. The Silnutzer bounds depend upon an integral ζ_2 which involves the three-point probability function S_3, where $S_n(\mathbf{r}_1,\ldots,\mathbf{r}_n)$ denotes the probability of finding n points at vector positions $\mathbf{r}_1,\ldots,\mathbf{r}_n$ all in one of the two phases, say phase 2. Milton's bounds depend also on ζ_2, but on the four-point probability function S_4. It is noteworthy

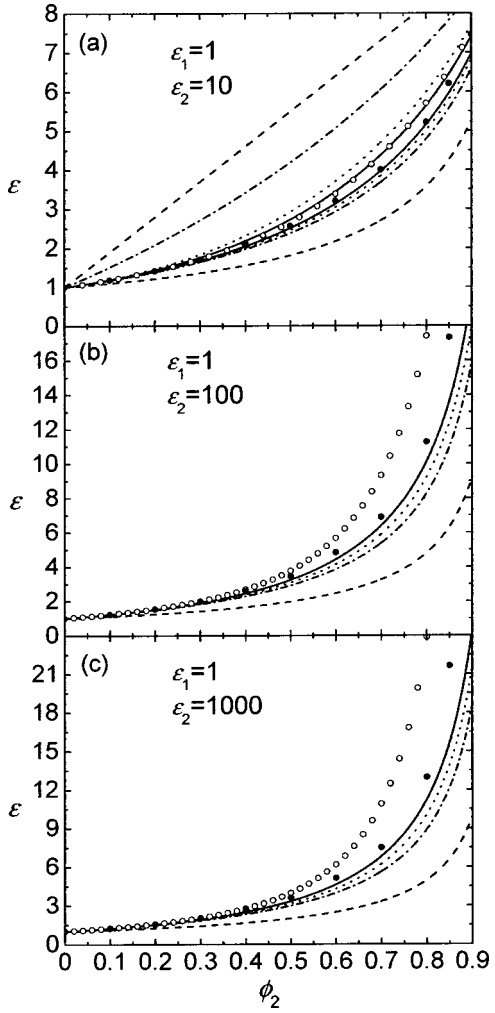

FIG. 10. The dependence of the bounds on ε as a function of the surface fraction ϕ_2 of disks for $\varepsilon_2/\varepsilon_1>1$. Dashed, dash-dotted, dotted, and solid curves correspond to the one-point, two-point, three-point, and four-point bounds, respectively, and the solid circles are obtained by FEM. Upper bounds are not shown in (b) and (c). For comparison, values of ε obtained from the Bruggeman equation are also represented by open circles.

that the three-point parameter ζ_2 has been computed for random-media models, including the random distribution of hard (impenetrable) disks in a matrix, by several investigators [24,78].

In the present paper, we used the values of the microstructural parameter ζ_2 which were obtained from the approximate relation $\zeta_2=\phi_2/3-0.05707\phi_2^2+O(\phi_2^3)$ [22]. To test the results, we now consider some specific examples. For a wide range of the permittivity ratio $\varepsilon_1/\varepsilon_2 \ll 1$, Figs. 10(a)–10(c) display a comparison of upper and lower bounds on the effective permittivity and the calculated data in the present work. Figure 10 indicates that the fourth-order bounds are narrower than the third-order bounds which significantly improve upon first-order and second-order bounds. Figure 10 also shows that the fourth-order lower bound provides an excellent estimate of the effective permittivity for a wide range of surface fractions up to $\phi_2 \cong 0.7$, in agreement with the fact that the bounds become progressively narrower as

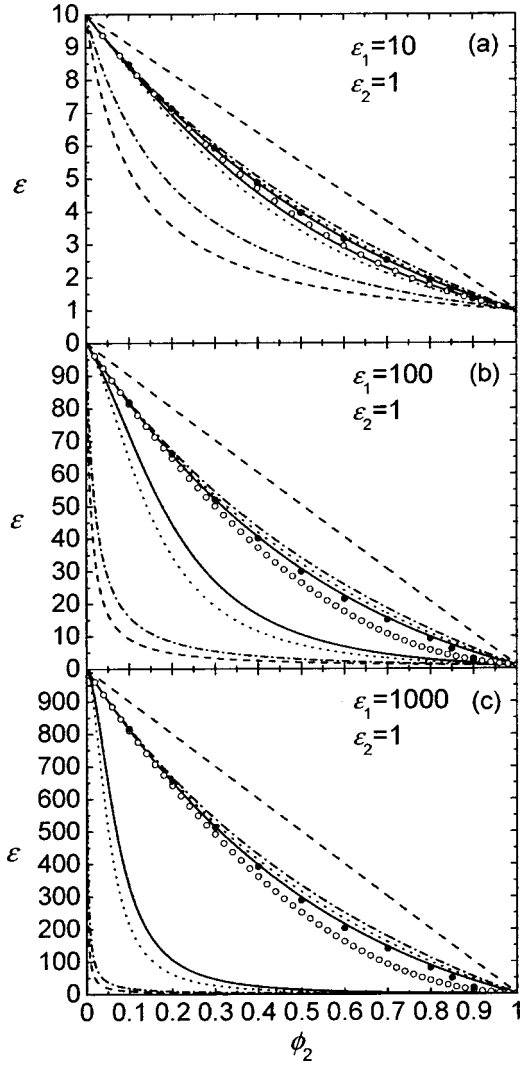

FIG. 11. Same as in Fig. 10 for $\varepsilon_2/\varepsilon_1<1$.

more microstructural information is incorporated [24,79].

Fig. 11 is analogous to Fig. 11 but for $\varepsilon_1/\varepsilon_2 \gg 1$. In Fig. 11, the same trend can be observed in the comparison of bounds with the numerical data, i.e., the fourth-order upper bound provides a good estimate of the calculated data. However, it is quite remarkable that the upper second-order, third-order, and fourth-order bounds are very close to each other, the accuracy of the bound increasing as the order increases.

E. Comparison with exact results concerning regular arrays

Following the check on bounds of ε, we present illustrative results from simulations for regular arrays, i.e., cases for which an exact solution can be derived. Note that this geometry renders the two-component composite materials translationally and rotationally invariant. As a standard of comparison, we present in Fig. 12 plots of the scaled permittivity $\varepsilon/\varepsilon_1$ for regular arrays of 2D identical circular disks embedded in a uniform matrix, as a function of the disks surface fraction ϕ_2 at values of the permittivity ratio $\varepsilon_2/\varepsilon_1$=10, 50, and ∞, respectively. We observe that the results from the two

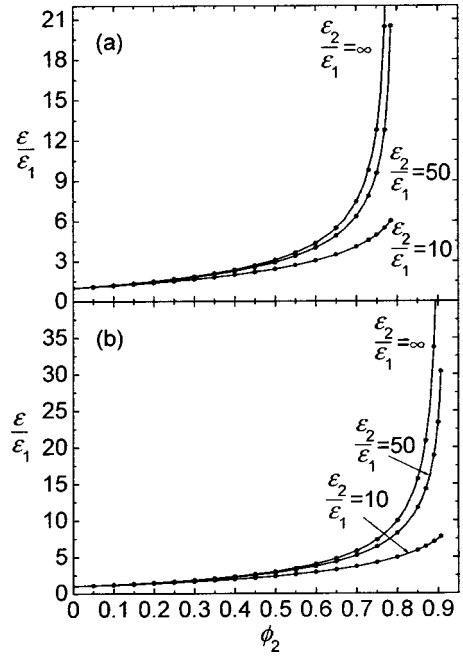

FIG. 12. Comparison of the FEM simulation data (filled symbols) for the normalized effective permittivity $\varepsilon/\varepsilon_1$ of 2D arrays of a disk with the prediction from exact models [31,80]. The three curves correspond, respectively, to $\varepsilon_2/\varepsilon_1$=10, 50, and ∞. (a) Square array, (b) hexagonal array.

methods, FEM and analytical [80], compare almost exactly with each other, validating the accuracy of the FEM method.

F. Comparative assessment of the FEM approach with equations for predicting the effective permittivity of heterogeneous media

In this subsection, the performance of the FEM approach is compared to that of four common equations for predicting the effective permittivity of inhomogeneous media. It is worth observing that the role of analytical models is different from, and complementary to, that of detailed numerical simulations. Simulations are virtual experiments. However, they are limited, even with the fastest computers, to exploring relatively short time and length scales. Analytical models are typically simpler and more approximate, but they can give direct insights into how materials properties arise from microscopic interactions. Moreover, analytical models can often treat a broad range of conditions, reveal trends, suggest functional relations for engineering applications, and motivate experiments. A number of analytical equations to calculate the effective permittivity for a wide variety of condensed-matter systems have been reported; see Refs. [81,82], and references cited therein. For physical problems in particular, there has been a long history of mixing laws for composite materials, provided the constituent material phases do not chemically react with each other. However, this set of approximations is primarily viewed as an ansatz: a set of practical, useful, yet somewhat heuristic prescriptions for estimating dielectric properties of heterostructures. Although an empirical description has limited transferability,

and its ability to give quantitative results should always be carefully scrutinized, such an approach can be quite useful in exploratory studies. The underlying physics of nearly all EMT models revolve around one or a combination of two principal elements: (1) because of the difficulties in dealing with multiple length scales, a practical approach to study such systems is coarse-graining, i.e., reducing problem to an effective one-component system of particles interacting through the effective potential, and (2) the free-space wavelength of the field is assumed to be much larger than the scale of inhomogeneities in the composite. We have already used this approach to fit the microwave dielectric response of carbon black-filled polymers over a wide range of carbon black concentrations [83]. This approach is more subjective than one would hope for and has led to much discussion in the literature [17,33,83]. Given the above complexities, it is clear that there is strong motivation to move beyond reduced mean-field approaches and to attempt a statistical treatment of the system.

Keeping the same notation as above, ε, ε_1, and ε_2 denote, respectively, the effective permittivity of the composite material, the permittivity of the matrix with surface fraction ϕ_1, and the permittivity of the inclusion phase with a surface fraction ϕ_2. The most popular mixing laws and EMT are those of Maxwell-Garnett,

$$\varepsilon = \varepsilon_1 \frac{\varepsilon_1\phi_1(1-A) + \varepsilon_2(\phi_2 + A\phi_1)}{\varepsilon_1 + A\phi_1(\varepsilon_2 - \varepsilon_1)}, \tag{3.3}$$

Böttcher (also termed symmetric Bruggeman),

$$\varepsilon = \varepsilon_1 + (\varepsilon_2 - \varepsilon_1)\phi_2 \frac{\varepsilon}{\varepsilon + (\varepsilon_2 - \varepsilon)A}, \tag{3.4}$$

Bruggeman (asymmetric),

$$\frac{\varepsilon - \varepsilon_2}{\varepsilon_1 - \varepsilon_2}\left(\frac{\varepsilon_1}{\varepsilon}\right)^A = \phi_1, \tag{3.5}$$

and Looyenga,

$$\varepsilon^{1-2A} = \phi_1\varepsilon_1^{1-2A} + \phi_2\varepsilon_2^{1-2A}, \tag{3.6}$$

where $A(0 \leqslant A \leqslant 1)$ is the depolarization factor which depends on the shape of the inclusions. For disks $A = \frac{1}{2}$.

In order for the assessment to be reliable, calculations of the effective permittivity should be performed with different permittivity ratios $\varepsilon_2/\varepsilon_1$. Figures 13 and 14 display the numerical data of the current work superposed with the predictions of Eqs. (3.3)–(3.6). Based on the results shown in Figs. 13 and 14, we see that for ϕ_2 below 0.4, our data approach the theoretical models as expected, i.e., the dilute limit [22]. As seen in these figures, Bruggeman's asymmetrical model is superior to the other models in the prediction of ε, particularly for ϕ_2 above 0.4. In all cases, the Bottcher and Looyenga equations have been shown to have poor predictive ability for hard disk distributions at high surface fraction and both for very large, i.e., Figs. 13(a)–13(c), and very small, i.e., Figs. 14(a)–14(c), permittivity ratios. This is of fundamental importance because higher multipole interactions become important when the inclusions approach contact. EMT as previously formulated certainly break down at high volume fractions of inclusions since they are based on a dipolar analysis, and do not take into account the multipole interactions contributing to the polarization of the material medium. The same higher multipole interactions that produce the permittivity increase (Fig. 13) or decrease (Fig. 14) also enforce disk clustering. This confines and localizes higher multipole effects to the close-packed clustered regions.

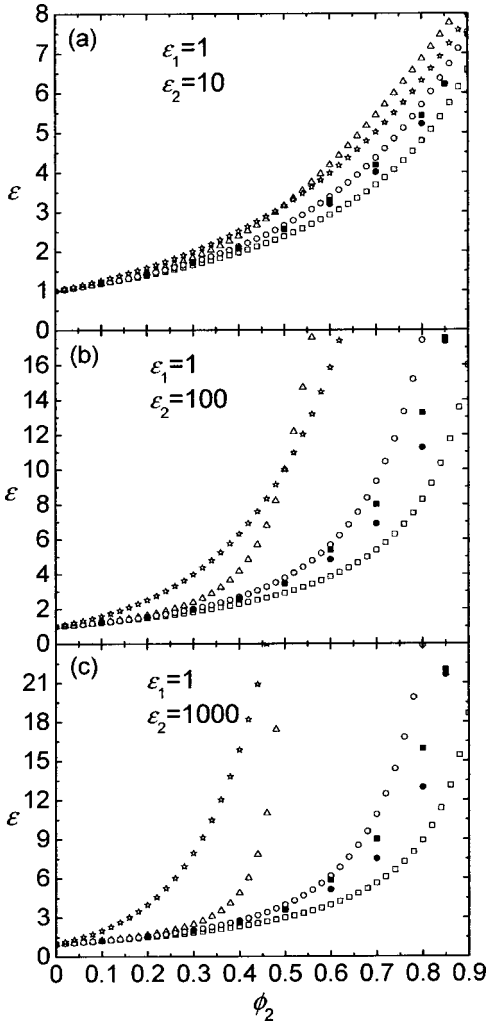

FIG. 13. Comparison of the FEM simulation data (filled circles) for ε of random distributions of disks with $\varepsilon_2/\varepsilon_1 > 1$. Open squares, circles, triangles, and stars represent Maxwell Garnett, Bruggeman, Böttcher, and Looyenga formulas, respectively. For comparison, the filled squares denote the corresponding value of the permittivity for a nonequilibrium configuration.

Figures 13 and 14 show also for comparison the values of ε calculated for a given nonequilibrium distribution of hard disks, i.e., distribution which is not equilibrated by MC runs. Here, it should be recalled that for $\phi_2 \leqslant \phi_2^{sat}$, we used the RSA process for the random distribution of disks, whereas Clarke and Wiley's algorithm was used for higher surface fractions. Three comments are in order. First, we observe that the values of ε calculated with the RSA process and those corresponding to equilibrium distributions are identical for surface fractions $\phi_2 \leqslant 0.5$. This is quite surprising since one would expect that exclusion surface effects imply very different results between the RSA-obtained and equilibrium dis-

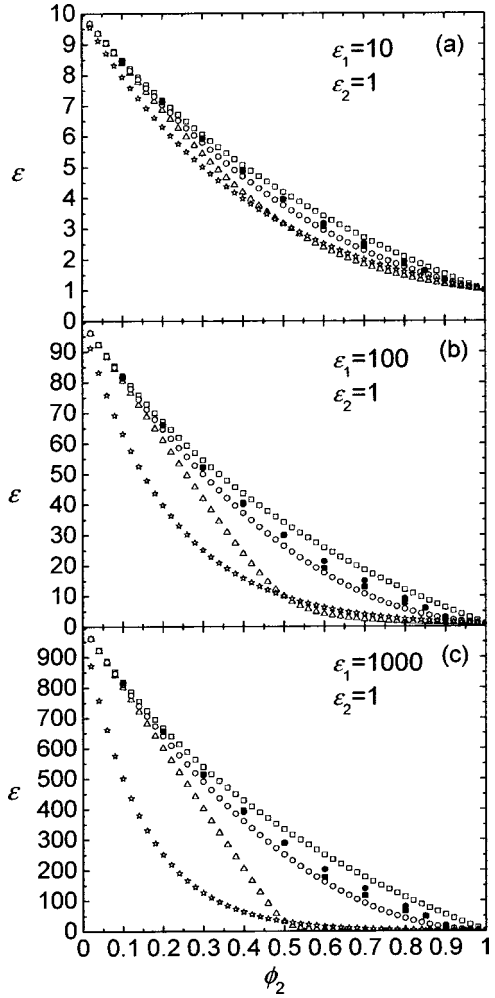

FIG. 14. Same as in Fig. 13 for $\varepsilon_2/\varepsilon_1<1$.

tributions. For higher surface fractions, the values of ε for the nonequilibrium distribution are larger than the equilibrium one, and the difference between these values increases monotonically as the surface fraction is increased. This may be due to the following fact: at equilibrium, the disks are uniformly distributed in a surface, whereas in the nonequilibrium distribution clusters of disks can be formed leading to larger values of ε. From a practical point of view, we must be aware that the calculated values of ε for nonequilibrium distributions for $\phi_2 > \phi_2^{sat}$ are very sensitive to the algorithm which is used for generating the initial configuration. Figures 13 and 14 show also that, as the surface fraction of disks approaches the close packing fraction, the difference between equilibrium and nonequilibrium values of ε tends to decrease because of the large entropy decrease of the system. Second, and in like fashion as the equilibrium situation, the values of ε calculated for the nonequilibrium distribution are between those obtained from the Maxwell-Garnett and Bruggeman formulas. Third, we also verified (not displayed in the figures) that the nonequilibrium values of ε are within the fourth-order bounds calculated for the equilibrium distribution, in agreement with the facts that the RSA-obtained and the equilibrium distributions are identical at the level of the third virial coefficient, and that the value of the three-point microstructure parameter ζ_2 which is used for the calculations of bounds for the equilibrium distribution is also exact for the RSA distribution [79].

Results from the Bruggeman equation are also shown in Figs. 10 and 11 for comparison. The deviations between Bruggeman values and those obtained from upper and lower bounds increase for very large and very small permittivity ratios. It is noted that the results reported here are in good agreement with the results of Kärkkäinen and co-workers [84], who found effective permittivity data of a 2D mixture calculated by the FDTD method in between the predictions of the Maxwell-Garnett and Bruggeman equations. These insights may help to explain the polarization mechanisms which characterize the dispersion behavior in heterostructures with broken-translational symmetry.

IV. CONCLUDING SECTION

We are now ready to summarize the results of the preceding section and conclude with some comments concerning several open questions.

A. Summary

We have made two contributions with this paper. The first one is general in nature, and consists in a versatile FEM simulation approach, in the context of 2D applications, for quantifying simultaneously structural descriptors such as the mean coordination number and RDF, and the effective permittivity, regardless of which mechanism causes internal disorder. An understanding of the morphology is a prerequisite to being able to tune the dielectric behavior of composite structures. A reliable algorithm of easy implementation and wide applicability was presented that (1) prepares equilibrated configurations of disks in a background matrix, and (2) solves the equations of continuum electrostatics for systems of heterogeneous permittivity in random sample realizations. From our previous experience, it is important to note that a critical aspect for the success of any sequential method concerns the manner in which the packing construction is done. We should not leave this part of our presentation without reminding the reader that our method introduces a geometric parameter δ which defines a minimum separation distance between the inclusions. The results do not answer the question of what is the optimal value for δ, and it should be evaluated on case-by-case basis. This study focused some of the practical issues confronted when performing FEM and MC simulations, e.g., the number of MC steps needed to achieve equilibrium.

The second contribution from the current work is specific, and consists of a set of information from FEM simulations for random mixtures of two constituents with different permittivities. We have demonstrated the efficiency of our method by applying it to a number of test cases. Collectively, all of the above simulation results assess the accuracy of the calculated values of the permittivity for 2D lossless systems and agree fairly well with the results already available in the literature. Our calculations confirm the general rules that the bounds become progressively narrower as more microstructural information is incorporated, but the methodology that

we present is also useful for examining those cases for which the general rules do not apply. Such a comparison is critical in order to ascertain the numerical scheme accuracy, the range of applicable inclusion surface fractions, and to guide future improvements. As far as we know, there are no available experimental data with which to compare the predicted dielectric behavior of these heterostructures. Our hope is that this computer simulation will serve as a test case for those investigators who work in the subject of electromagnetic properties of random heterogeneous materials.

B. Outlook

What is the future outlook? There are several nontrivial extensions of the current work that would be interesting and which deserve future consideration. We have restricted ourselves to discussing the 2D nondissipative case, i.e., rigid disks in the plane and ε is real, but the real-space approach we have described is more general, and is generalizable beyond the simple model proposed here to more realistic 3D lossy media. This will provide the opportunity to identify similarities and contrasts with the 2D case. The method lends itself to the study of more general systems. For example, we note that we have assumed equal radii for the disks. An issue which is of interest in random disk packing studies is to include in the simulations species with different diameters, i.e., polydispersity with two or three different diameters or with a continuous spread of disk diameters. Another direction would be to consider a more elaborate particle shape, e.g., ellipse, for which the local orientational order will doubtless affect the permittivity of random packings. Because of the above-presented mathematical analogy, the present results are also relevant to the determination of other relevant macroscopic (effective) quantities such as the effective thermal conductivity and magnetic permeability of random multiphase systems [4,9].

ACKNOWLEDGMENTS

The financial support of the Conseil Général du Finistère to V.M. is gratefully acknowledged. The authors are also grateful to Professor Fred Lado from the Physics Department, at North Carolina State University, Raleigh, for help with the calculation of the RDF from the PY equation. The Laboratoire d'Électronique et Systèmes de Télécommunications is Unité Mixte de Recherche CNRS 6165.

APPENDIX

This appendix is meant to summarize *a priori* estimates of upper, i.e., $\varepsilon_U^{(i)}$, and lower, i.e., $\varepsilon_L^{(i)}$, bounds for ε which have been used for comparison with the FEM results. As noted in the Introduction, for such descriptions, a number of authors have developed various approaches delivering different levels of sophistication and predictive power. These estimates narrow the composition range of possible effective permittivity. Detailed treatments can be found in the references.

The loosest and simplest bounds are the so-called Wiener one-point bounds [85],

$$\varepsilon_L^{(1)} = (\varepsilon_1^{-1}\phi_1 + \varepsilon_2^{-1}\phi_2)^{-1},$$

$$\varepsilon_U^{(1)} = \varepsilon_1\phi_1 + \varepsilon_2\phi_2. \tag{A1}$$

Hashin-Shtrikman two-point bounds [74] for any d-dimensional two-phase isotropic mixture in which $\varepsilon_2 \geqslant \varepsilon_1$ are

$$\varepsilon_L^{(2)} = \varepsilon_1\phi_1 + \varepsilon_2\phi_2 - \frac{\phi_1\phi_2(\varepsilon_2-\varepsilon_1)^2}{\varepsilon_1\phi_2 + \varepsilon_2\phi_1 + (d-1)\varepsilon_1},$$

$$\varepsilon_U^{(2)} = \varepsilon_1\phi_1 + \varepsilon_2\phi_2 - \frac{\phi_1\phi_2(\varepsilon_2-\varepsilon_1)^2}{\varepsilon_1\phi_2 + \varepsilon_2\phi_1 + (d-1)\varepsilon_2}. \tag{A2}$$

The three-point bounds on effective permittivity [75,77] of any d-dimensional two-phase isotropic heterogeneous media are

$$\varepsilon_L^{(3)} = \varepsilon_1\phi_1 + \varepsilon_2\phi_2 - \frac{\phi_1\phi_2(\varepsilon_2-\varepsilon_1)^2}{\varepsilon_1\phi_2 + \varepsilon_2\phi_1 + (d-1)(\varepsilon_1^{-1}\phi_1 + \varepsilon_2^{-1}\phi_2)^{-1}},$$

$$\varepsilon_U^{(3)} = \varepsilon_1\phi_1 + \varepsilon_2\phi_2 - \frac{\phi_1\phi_2(\varepsilon_2-\varepsilon_1)^2}{\varepsilon_1\phi_2 + \varepsilon_2\phi_1 + (d-1)(\varepsilon_1\zeta_1 + \varepsilon_2\zeta_2)}, \tag{A3}$$

where $\zeta_1+\zeta_2=1$.

Milton [6,71] derived four-point bounds on the effective permittivity isotropic two-phase composite for which $\varepsilon_2 \geqslant \varepsilon_1$,

$$\frac{\varepsilon_L^{(4)}}{\varepsilon_1} = \frac{1 + [(d-1)\phi_2 - \gamma_2/\zeta_2]\beta_{21} + (1-d)[\phi_1\zeta_2 + \phi_2\gamma_2/\zeta_2]\beta_{21}^2}{1 - [\phi_2 + \gamma_2/\zeta_2]\beta_{21} + [\phi_1(1-d)\zeta_2 + \phi_2\gamma_2/\zeta_2]\beta_{21}^2},$$

$$\frac{\varepsilon_U^{(4)}}{\varepsilon_2} = \frac{1 + [(d-1)\phi_1 - \gamma_1/\zeta_1]\beta_{12} + (1-d)[\phi_2\zeta_1 + \phi_1\gamma_1/\zeta_1]\beta_{12}^2}{1 - [\phi_1 + \gamma_1/\zeta_1]\beta_{12} + [\phi_2(1-d)\zeta_1 + \phi_1\gamma_1/\zeta_1]\beta_{12}^2}, \tag{A4}$$

where $\gamma_1-\gamma_2=(d-2)(\zeta_2-\zeta_1)$ and $\beta_{ij}=(\varepsilon_i-\varepsilon_j)/[\varepsilon_i+(d-1)\varepsilon_j]$, $i\neq j$. These four-point bounds depend upon ϕ_i, ζ_i, and the four-point parameters γ_i. It is interesting to note that, making use of the phase interchange theorem, Milton showed that γ_i can be expressed in terms of ϕ_2 and ζ_2.

[1] L. K. H. van Beek, Prog. Dielectr. **7**, 67 (1967).

[2] A. H. Sihvola, *Electromagnetic Mixing Formulas and Applications* (IEE Publishing, London, 1999).

[3] D. K. Hale, J. Mater. Sci. **11**, 2105 (1976).

[4] G. K. Batchelor, Annu. Rev. Fluid Mech. **6**, 227, 1974.

[5] S. Redner, *Physics of Finely Divided Matter* (Springer-Verlag, Berlin, 1985).

[6] G. W. Milton, J. Appl. Phys. **52**, 5294 (1981). See also G. W. Milton, *The Theory of Composites* (Cambridge University Press, Cambridge, 2002).

[7] R. G. Parr and W. Yang, *Density-Functional Theory of Atoms and Molecules* (Oxford University Press and Clarendon Press, New York and Oxford, 1989).

[8] O. C. Zienkiewicz and R. L. Taylor, *The Finite Element Method* (McGraw-Hill, New York, 1994).

[9] C. Brosseau and A. Beroual, Prog. Mater. Sci. **48**, 373 (2003).

[10] V. Rokhlin, J. Comput. Phys. **60**, 187 (1985).

[11] J. Helsing, J. Math. Phys. **36**, 2941 (1995).

[12] J. M. Haile, C. Massobrio, and S. Torquato, J. Chem. Phys. **83**, 4075 (1985). See also J. M. Haile, *Molecular Dynamics Simulation: Elementary Methods* (Wiley, New York, 1992).

[13] S. Stölzle, A. Enders, and G. Nimtz, J. Phys. I **2**, 401 (1992). See also T. Weiland, Part. Accel. **17**, 227 (1985); T. Weiland, *ibid.* **15**, 245 (1984).

[14] K. Binder and D. W. Heermann, *Monte Carlo Simulation in Statistical Physics* (Springer-Verlag, Berlin, 1988). Molecular dynamics, which uses a deterministic approach, gives information about the time evolution of a system. On the other hand, Monte Carlo methods are stochastic in nature and are useful in understanding the system in equilibrium.

[15] A. W. Appel, SIAM (Soc. Ind. Appl. Math.) J. Sci. Stat. Comput. **6**, 85 (1985).

[16] J. Carrier, L. Greengard, and V. Rokhlin, SIAM (Soc. Ind. Appl. Math.) J. Sci. Stat. Comput. **9**, 669 (1988). See also L. Greengard and V. Rokhlin, *The Rapid Evaluation of Potential Fields in Three Dimensions* (MIT Press, Cambridge, MA, 1988). Using the multipole method, proposed by Greengard and Rokhlin, to solve an electrostatic problem with the boundary element method reduces the computational cost and the memory requirements from $O(M^2)$ to $O(M)$, where M is the number of unknowns.

[17] I. A. Youngs, J. Phys. D **35**, 3127 (2002).

[18] K. K. Kärkkäinen, A. H. Sihvola, and K. I. Nikoskinen, IEEE Trans. Geosci. Remote Sens. **38**, 1303 (2000); **39**, 1013 (2001). See also K. L. Shlager, and J. B. Schneider, IEEE Antennas Propag. Mag. **37**, 39 (1995). See also K. S. Kunz and R. J. Luebbers, *The FDTD Method for Electromagnetics* (CRC, Boca Raton, FL, 1993) and K. L. Shlager and J. B. Schneider, IEEE Antennas Propag. Mag. **37**, 39 (1995).

[19] H. Ma, B. Zhang, W. Y. Tam, and P. Sheng, Phys. Rev. B **61**, 962 (2000). See also J. C. Michel, H. Moulinec, and P. Suquet, Comput. Mod. Eng. Sci. 1, 79 (2000).

[20] D. J. Bergman and K.-J. Dunn, Phys. Rev. B **45**, 13262 (1992).

[21] R. Tao, Z. Chen, and P. Sheng, Phys. Rev. B **41**, 2417 (1990).

[22] S. Torquato, *Random Heterogeneous Materials: Microstructure and Macroscopic Properties* (Springer, New York, 2002).

[23] I. C. Kim and S. Torquato, J. Appl. Phys. **68**, 3892 (1990).

[24] S. Torquato, T. M. Truskett, and P. G. Debenedetti, Phys. Rev. Lett. **84**, 2064 (2000).

[25] R. M. German, *Particle Packing Characteristics* (Metal Powder Industries Federation, Princeton, NJ, 1989).

[26] J. C. Maxwell, *Treatise on Electricity and Magnetism* (Clarendon, Oxford, 1873), p. 194.

[27] D. A. G. Bruggeman, Ann. Phys. (Leipzig) **24**, 636 (1935).

[28] C.-W. Nan, Prog. Mater. Sci. **37**, 1 (1993).

[29] D. Bergman and D. Stroud, *Solid State Physics, Advances in Research and Applications*, edited by H. Ehrenreich and D. Turnbull (Academic, San Diego, 1992), Vol. 46, p. 147.

[30] A. Lagarkov and A. K. Sarychev, Phys. Rev. B **53**, 6318 (1998). See also A. N. Lagarkov, S. M. Matytsin, K. N. Rozanov, and A. K. Sarychev, Physica A **241**, 58 (1997).

[31] M. Sahimi, *Heterogeneous Materials I: Linear Transport and Optical Properties* (Springer, New York, 2003).

[32] W. T. Doyle, J. Appl. Phys. **49**, 795 (1978). See also E. R. Smith and V. Tsarenko, Mol. Phys. **95**, 449 (1998) for a detailed study of the convergence of multipole expansion methods.

[33] Readers interested in the details of the phenomenology behind the GEMT equation can find a comprehensive description of its development and application to composites in the following set of papers: D. S. McLachlan, Solid State Commun. **72**, 831 (1989); J. Hwang, D. S. McLachlan, and T. O. Mason, J. Electroceram. **3**, 7 (1999); D. S. McLachlan, J. Hwang, and T. O. Mason, *ibid.* **5**, 37 (2000); and D. S. McLachlan, M. Blaszkiewics, and R. E. Newnham, J. Am. Chem. Soc. **73**, 2187 (1990).

[34] J. P. Hansen and I. R. McDonald, *Theory of Simple Liquids* (Academic, London, 1976).

[35] J. G. Berryman, Phys. Rev. A **27**, 1053 (1983).

[36] J. D. Bernal, Proc. R. Soc. London, Ser. A **280**, 299 (1964).

[37] P. M. Chaikin and T. C. Lubensky, *Principles of Condensed Matter Physics* (Cambridge University Press, Cambridge, 1998).

[38] S. Chapman and T. G. Cowling, *The Mathematical Theory of Non-Uniform Gases* (Cambridge University Press, Cambridge, 1953).

[39] T. D. Lee, K. Huang, and C. N. Yang, Phys. Rev. **106**, 1135 (1957). See also K. Huang and C. N. Yang, *ibid.* **105**, 767 (1957).

[40] C. A. Rogers, *Packing and Covering* (Cambridge University Press, Cambridge, 1964).

[41] F. P. Buff and F. H. Stillinger, J. Chem. Phys. **39**, 1911 (1963).

[42] A. P. Roberts, Phys. Rev. E **56**, 3203 (1997).

[43] For example, transport properties in polymer carbon black composites depend on the whole structure which needs to be described at all length scales from the primary aggregates size (a few tens of nanometers) up to micrometers. TEM and atomic force microscopy coupled with image analysis have been widely used to examine morphological parameters characterizing the dispersion state, e.g., distribution of aggregate size and interaggregate distances in the matrix, in investigation of their effects on the properties of filled polymers. However, it is well established that the use of microscopy for the quantitative study of these parameters may present difficulties arising from the fact that it provides only 2D information, i.e., A. C. Roulin-Moloney, *Fractography and Failure Mechanisms of Polymers and Composites* (Elsevier, London, 1989), and C. Brosseau, P. Molinié, F. Boulic, and F. Carmona, J. Appl. Phys. **89**, 8297 (2001).

[44] N. Metropolis, A. W. Rosenbluth, M. N. Rosenbluth, A. H. Teller, and E. Teller, J. Chem. Phys. **21**, 1087 (1953). See also M. Kalos and P. Whitlock, *Monte Carlo Methods* (Wiley-Interscience, New York, 1986), and *A Guide to Monte Carlo Simulations in Statistical Physics*, edited by D. P. Landau and K. Binder (Springer-Verlag, Berlin, 1986).
[45] B. Widom, J. Chem. Phys. **44**, 3888 (1966).
[46] A. S. Clarke and J. D. Wiley, Phys. Rev. B **35**, 7350 (1987).
[47] B. D. Lubachevsky and F. H. Stillinger, J. Stat. Phys. **60**, 561 (1990). See also B. D. Lubachevsky, F. H. Stillinger, and E. N. Pinson, *ibid.* **64**, 501 (1994).
[48] C. H. Bennett, J. Appl. Phys. **43**, 2727 (1972).
[49] D. J. Adams and A. J. Matheson, J. Chem. Phys. **56**, 1989 (1972).
[50] W. M. Visscher and M. Bolsterli, Nature (London) **239**, 504 (1972).
[51] J. L. Finney, Mater. Sci. Eng. **23**, 199 (1976).
[52] E. L. Hinrichsen, J. Feder, and T. Jossang, Phys. Rev. A **41**, 4199 (1990).
[53] I. Krakovsky and V. Myroshnychenko, J. Appl. Phys. **92**, 6743 (2002).
[54] F. H. Stillinger, E. A. DiMarzio, and R. L. Kornegay, J. Chem. Phys. **40**, 1564 (1964).
[55] M. Shahinpoor, Powder Technol. **25**, 163 (1980).
[56] T. J. Quickenden and G. K. Tan, J. Colloid Interface Sci. **48**, 382 (1974).
[57] H. H. Kausch, D. G. Fesko, and N. W. Tschoegl, J. Colloid Interface Sci. **37**, 603 (1971).
[58] D. N. Sutherland, J. Colloid Interface Sci. **60**, 96 (1977).
[59] M. Sugiyama, Prog. Theor. Phys. **63**, 1848 (1980).
[60] MATLAB 6.5, The MathWorks, Inc., 2002.
[61] http://www.mathworks.com/support/solutions/data/8542.shtml
[62] FEMLAB 2.3b, Comsol, Stockholm, Sweden, 2003.
[63] F. Zernike and J. A. Prins, Z. Phys. **41**, 184 (1927); K. F. Herzfeld and M. G. Mayer, J. Chem. Phys. **2**, 38 (1934); L. Tonks, Phys. Rev. **50**, 955 (1936).
[64] Y. Uehara, T. Ree, and F. H. Ree, J. Chem. Phys. **70**, 1876 (1979).
[65] J. Tobochnik and P. M. Chapin, J. Chem. Phys. **88**, 5824 (1988).
[66] Y. Song, R. M. Stratt, and E. A. Mason, J. Chem. Phys. **88**, 1126 (1988).
[67] J. B. Keller, J. Appl. Phys. **34**, 991 (1963). See also J. B. Keller, J. Math. Phys. **5**, 548 (1964).
[68] A. M. Dykhne, Zh. Eksp. Teor. Fiz. **59**, 110 (1970) [Sov. Phys. JETP **32**, 63 (1970)].
[69] K. S. Mendelson, J. Appl. Phys. **46**, 918 (1975); **46**, 4740 (1975).
[70] B. Ya. Balagurov, Zh. Eksp. Teor. Fiz. **81**, 665 (1981) [Sov. Phys. JETP **54**, 355 (1981)].
[71] G. W. Milton, Phys. Rev. Lett. **46**, 542 (1981); G. W. Milton, J. Appl. Phys. **52**, 5294 (1981); G. W. Milton, in *Physics and Chemistry of Porous Media*, edited by D. L. Johnson and P. N. Sen (American Institute of Physics, New York, 1984), and G. W. Milton, Commun. Math. Phys. **111**, 281 (1987).
[72] P. P. Durand and L. H. Ungar, Int. J. Numer. Methods Eng. **26**, 2487 (1988).
[73] K. A. Schulgasser, Int. Commun. Heat Mass Transfer **19**, 639 (1992).
[74] Z. Hashin and S. Shtrikman, J. Appl. Phys. **33**, 3125 (1962).
[75] M. J. Beran, *Statistical Continuum Theories* (Wiley, New York, 1968). See also M. J. Beran, Nuovo Cimento **38**, 771 (1965).
[76] D. J. Bergman, Phys. Rep. **43**, 377 (1978).
[77] N. Silnutzer, Ph.D. thesis, University of Pennsylvania, Philadelphia (1972).
[78] L. Greengard and J. Helsing, J. Appl. Phys. **77**, 2015 (1995).
[79] P. A. Smith and S. Torquato, J. Appl. Phys. **65**, 893 (1989).
[80] W. T. Perrins, D. R. McKenzie, and R. C. McPhedran, Proc. R. Soc. London, Ser. A **369**, 207 (1979).
[81] E. Tuncer, Y. V. Serdyuk, and S. M. Gubanski, IEEE Trans. Dielectr. Electr. Insul. **9**, 809 (2002).
[82] R. Landauer, in *Electrical Transport and Optical Properties of Inhomogeneous Media*, edited by J. C. Garland and D. B. Tanner, AIP Conf. Proc. No. 40 (AIP New York, 1978), p. 2 See also R. Landauer, J. Appl. Phys. **23**, 779 (1952).
[83] C. Brosseau, J. Appl. Phys. **91**, 3197 (2002).
[84] O. Pekonen, K. Kärkkäinen, A. Sihvola, and K. Nikoskinen, J. Electromagn. Waves Appl. **13**, 67 (1999).
[85] O. Wiener, Abh. Math.-Phys. Kl. Königl. Säcsh. Gesel. Wissen. 32, 509 (1912).